IOP Publishing | Royal Swedish Academy of Sciences Physica Scripta
Phys. Scr. 89 (2014) 044005 (5pp) doi:10.1088/0031-8949/89/04/044005

Extended x-ray absorption fine structure spectroscopy and first-principles study of $SnWO_4$

A Kuzmin[1], A Anspoks[1], A Kalinko[1,2], J Timoshenko[1] and R Kalendarev[1]

[1] Institute of Solid State Physics, University of Latvia, Kengaraga Street 8, LV-1063 Riga, Latvia
[2] Synchrotron SOLEIL, l'Orme des Merisiers, Saint-Aubin, BP 48, F-91192 Gif-sur-Yvette, France

E-mail: a.kuzmin@cfi.lu.lv

Received 6 June 2013, revised 26 September 2013
Accepted for publication 30 September 2013
Published 25 February 2014

Abstract
The local atomic structure in α- and β-$SnWO_4$ was studied by synchrotron radiation W L_3-edge x-ray absorption spectroscopy at 10 and 300 K. Strongly distorted WO_6 octahedra were found in α-$SnWO_4$, whereas nearly regular WO_4 tetrahedra were observed in β-$SnWO_4$, confirming previous results. The structural results obtained were supported by the first-principles calculations, suggesting that the second-order Jahn–Teller effect is responsible for octahedral distortion.

Keywords: tin tungstate, EXAFS, W L_3-edge, *ab initio* calculation, Jahn–Teller effect

(Some figures may appear in colour only in the online journal)

1. Introduction

Tin tungstate ($SnWO_4$) is an interesting compound, which has rarely been studied. It has two polymorphs (figure 1): the low-temperature orthorhombic α-phase (space group $Pnna$, no. 52) [1] and the high-temperature cubic β-phase (space group $P2_13$, no. 198) [2]. A diffusion-controlled phase transition occurs at 670 °C [2]; metastable (at room temperature) β-$SnWO_4$ can be prepared by a rapid quenching from above 670 °C [3]. The crystal structure of orthorhombic α-$SnWO_4$ [1] is composed of two-dimensional (2D) sheets of WO_6 octahedra, separated by layers of Sn^{2+} ions, which are six-fold coordinated by oxygens. The WO_6 octahedra within a sheet are joined by four corners and are distorted due to the second-order Jahn–Teller (SOJT) effect [4] because of the $W^{6+}(5d^0)$ electronic configuration. This distortion is associated with an off-center displacement of W^{6+} ions in the direction of the octahedron edge, so that there are three distinct W–O bonds (2×1.802, 2×1.889, 2×2.141 Å). The six-fold coordination of $Sn^{2+}(5s^26p^0)$ ions is distorted even more, leading to three different Sn–O bonds (2×2.184, 2×2.392, 2×2.826 Å). The pair of stereochemically active Sn 5s electrons is responsible for the 'lone pair' distortion of the SnO_6 octahedron via the SOJT effect [5].

The structure of cubic β-$SnWO_4$ is built up of slightly deformed WO_4 tetrahedra, which are interconnected with SnO_6 octahedra. The latter are strongly distorted via the SOJT effect [6] and have two different Sn–O bonds (3×2.214 and 3×2.810 Å) [2]. The WO_4 tetrahedra have three shorter (1.747 Å) and one longer (1.764 Å) W–O bonds: the bond length depends on how many tin atoms are bound to the oxygen atom. The distant oxygen atom in the WO_4 tetrahedron is shared with three tin atoms, whereas the other three oxygens bridge to one tin atom each.

The recent applicative interest in tin tungstate is caused by its possible use in day-light photocatalysis [5, 7–10] and gas sensors [11, 12]. It was found that β-$SnWO_4$ exhibits high visible-light photocatalytic activity in both microcrystalline ($d \sim 1\ \mu$m) and nanocrystalline ($d < 20$ nm) forms [5, 9, 10]. The photocatalytic performance of nanocrystalline α-$SnWO_4$ can be enhanced by Zn^{2+} doping, inducing band gap narrowing [13].

The photocatalytic activity of two tin tungstate phases is strongly related to their small band gaps (indirect $E_g = 1.64$ eV in α-$SnWO_4$ [5] and direct $E_g = 2.6$–2.7 eV in β-$SnWO_4$ [5, 6, 9]) and their unique band structures [5]. Results of density functional theory (DFT) calculations [5] suggest that the valence band in both tungstates is mainly composed of strongly interacting O 2p and Sn 5s states, whereas the conduction band has a W 5d–O 2p antibonding character with an admixture of Sn 5p states.

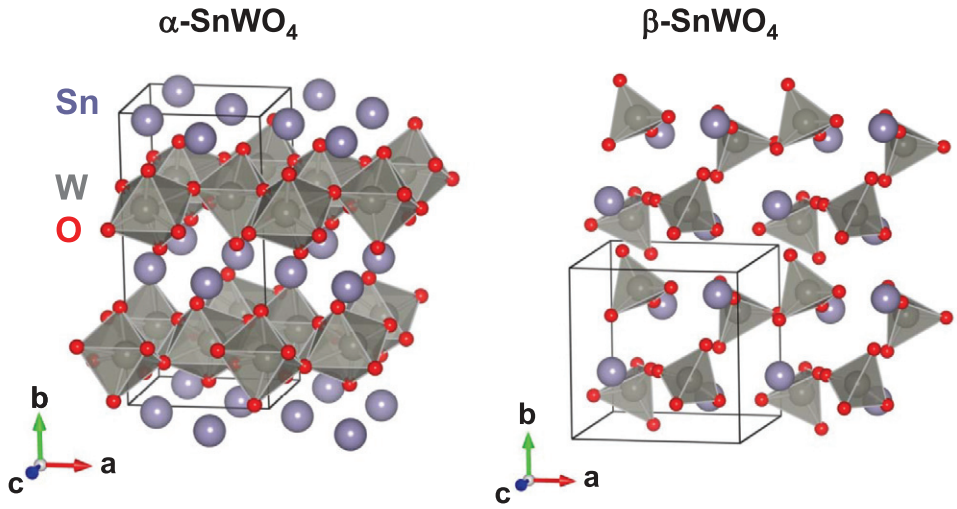

Figure 1. Crystal structure of α-$SnWO_4$ and β-$SnWO_4$. The unit cells are indicated.

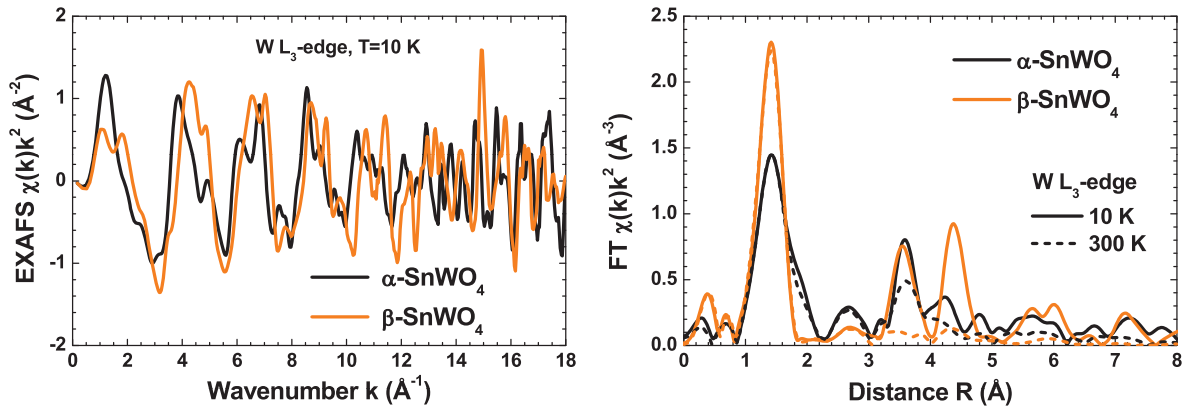

Figure 2. Experimental W L_3-edge EXAFS spectra $\chi(k)k^2$ (at 10 K) and their FTs (at 10 and 300 K) for α-$SnWO_4$ and β-$SnWO_4$.

In this study, we have used for the first time the W L_3-edge extended x-ray absorption fine structure (EXAFS) spectroscopy to probe the distortion of metal-oxygen octahedra in α-$SnWO_4$ and β-$SnWO_4$. The obtained results are complemented with those of the first-principles linear combination of atomic orbital (LCAO) calculations.

2. Experimental and calculation details

The synthesis of polycrystalline α-$SnWO_4$ and β-$SnWO_4$ was performed using the method described in [2, 3]. First, an equimolar amount of SnO (99.99%) and WO_3 (99.9%) powders was mixed and sealed in a silica ampoule under a vacuum. α-$SnWO_4$ was obtained by heating at 600 °C for 8 h, whereas β-$SnWO_4$ was produced by heating at 800 °C followed by rapid quenching down to room temperature.

The W L_3-edge (10 207 eV) x-ray absorption spectra were measured in transmission mode at the HASYLAB/DESY C (CEMO) bending magnet beamline [14] at room temperature. The radiation from the storage ring DORIS III was monochromatized by a detuned Si(111) double-crystal monochromator and its intensity was measured by two ionization chambers filled with argon and krypton gases.

The x-ray absorption spectra were analyzed using the EDA software package [15] following the conventional procedure [16, 17]. Fourier transforms (FTs) of the W L_3-edge EXAFS spectra $\chi(k)k^2$ for α-$SnWO_4$ and β-$SnWO_4$ are shown in figure 2. The first shell contributions into the total EXAFS spectra were isolated by Fourier filtering in the range of 0.8–2.2 Å; the radial distribution functions (RDFs) $G(R)$ for W–O bonds were obtained by the regularization-like method [18] (figure 3). Theoretical scattering amplitude and phase shift functions, employed in the EXAFS simulations, were calculated for α-$SnWO_4$ (β-$SnWO_4$) crystallographic structures [1, 2] by the self-consistent real space multiple-scattering (MS) FEFF8 code [19] using the complex exchange-correlation Hedin–Lundqvist potential [20] and the following values of the atomic muffin-tin radii: $R_{MT}(Sn) = 1.58$ Å (1.57 Å), $R_{MT}(W) = 1.23$ Å (1.14 Å) and $R_{MT}(O) = 0.93$ Å (0.92 Å) for α-$SnWO_4$ (β-$SnWO_4$).

The first-principles LCAO calculations were performed by the CRYSTAL09 code [21] using the hybrid exchange-correlation DFT/Hartree–Fock (HF) scheme. Such an approach was successfully used by us recently for other tungstates, such as $ZnWO_4$ [22, 23], $CaWO_4$ [23], $NiWO_4$ [24] and $CuWO_4$ [25]. Several hybrid functionals were tested and the best agreement with the experimental structure was obtained for the PBE0-13% functional [26] (the percentage defines the HF admixture in the exchange

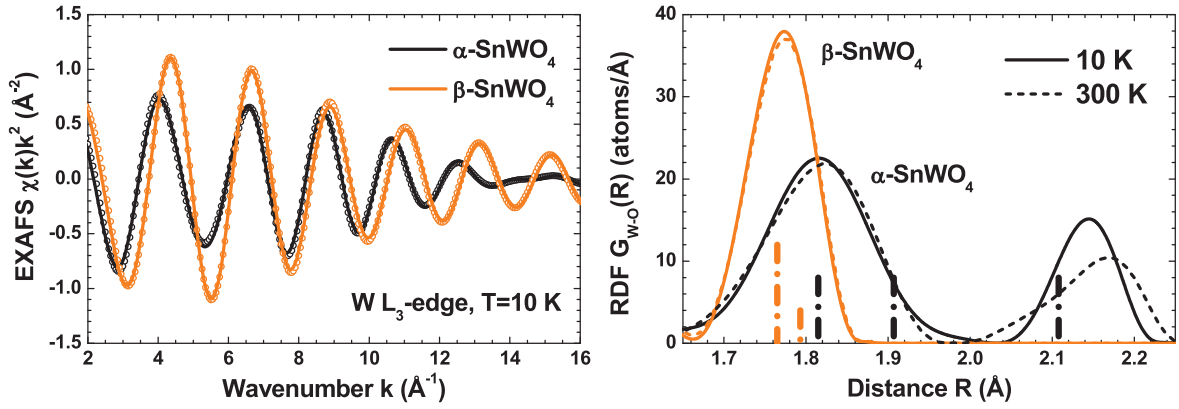

Figure 3. Left panel: experimental (circles) and calculated (solid lines) W L_3-edge EXAFS spectra $\chi(k)k^2$ at 10 K. Right panel: calculated RDFs $G(R)$ for W–O bonds within the first coordination shell of tungsten in α-$SnWO_4$ and β-$SnWO_4$ at 10 K (solid lines) and 300 K (dashed lines). The vertical columns indicate the position of the W–O distances, obtained by the LCAO calculations.

part of the DFT functional). Note that a similar result was previously found by us for $NiWO_4$ [24] and $CuWO_4$ [25]. The core electrons of the tungsten atoms were excluded from consideration using the Hay–Wadt effective small-core pseudopotential and the corresponding atomic basis set, excluding diffuse Gaussian-type orbitals. The Durand–Barthelat core pseudopotential, employed previously in the LCAO calculations of SnO_2 [27], and the corresponding atomic basis set have been used for tin atoms. The all-electron basis set, optimized in earlier calculations of perovskites [28], was employed for oxygen atoms. In the CRYSTAL09 code [21], the accuracy in evaluation of the Coulomb series and of the exchange series is controlled by a set of tolerances, which were taken to be (10^{-8}, 10^{-8}, 10^{-8}, 10^{-8}, 10^{-16}) H. The tolerance on the total energy change was set to 10^{-10} H. The Monkhorst–Pack scheme [29] for an $8\times8\times8$ k-point mesh in the Brillouin zone was applied.

3. Results and discussion

The low-temperature (10 K) experimental W L_3-edge EXAFS spectra $\chi(k)k^2$ for α-$SnWO_4$ and β-$SnWO_4$ are shown in figure 2. The high quality of experimental data and low thermal damping are responsible for the fact that the oscillations with large amplitudes are well observed even at high-k values. FTs of the EXAFS spectra, measured at 10 and 300 K, allow us to make several conclusions. First, the main contribution comes from the coordination shells, located at distances up to about 5 Å; however, the influence of the outer shells is also visible, especially at 10 K. The contribution from the first coordination shell (the peak at 1.4 Å), composed of six oxygen atoms, dominates and is weakly sensitive to the thermal disorder. The first shell peak is symmetric for β-$SnWO_4$, because the WO_4 tetrahedra are nearly regular. On the contrary, the distortion of the WO_6 octahedra in α-$SnWO_4$ is responsible for the asymmetric shape of the first shell peak, which is broadened and has a shoulder at 2 Å (figure 2).

The next peak in the FT at 2.7 Å is due to the MS effects generated within the first coordination shell. It has a small amplitude for the tetrahedral coordination of tungsten in β-$SnWO_4$, but has nearly a twice larger amplitude in the case of the octahedral coordination in α-$SnWO_4$, as expected [30]. The main contribution into this peak, coming from the scattering events within the O–W–O chains, increases when the value of the angle $O\widehat{W}O$ approaches 180°, i.e. the angle becomes linear and the intermediate tungsten atom strongly focuses the photoelectron wave [31]. In the tetrahedral case, WO_4 units in β-$SnWO_4$ all angles $O\widehat{W}O \approx 109°$, whereas there are two angles $O\widehat{W}O \approx 170°$ and one angle $O\widehat{W}O \approx 157°$ in the distorted WO_6 octahedra in α-$SnWO_4$.

The results of the MS calculations suggest that the group of peaks between 3 and 5 Å is due to the outer coordination shells, which are dominated by the shells containing metal atoms (Sn and W). In α-$SnWO_4$, the peak at 3.6 Å contains contributions from a group of six Sn atoms and four W atoms, whereas the peak at 4.2 Å includes a contribution from two Sn atoms. In β-$SnWO_4$, the peak at 3.6 Å contains contributions from seven Sn atoms, whereas the peak at 4.4 Å is due to six W atoms.

Opposite to the first shell, the outer shells are more sensitive to thermal disorder. The change of temperature from 10 to 300 K results in a decrease of both peaks between 3 and 5 Å in α-$SnWO_4$ and their complete disappearance for β-$SnWO_4$. Such behavior can be explained by the difference in the atomic structure of the two phases. The WO_4 units in β-$SnWO_4$ behave as rigid and are loosely connected with each other, as well as with the nearest SnO_6 units. On the contrary, the WO_6 units in α-$SnWO_4$ are bound to each other and form 2D sheets in the ac-plane.

Now we turn to a detailed analysis of the first coordination shell of tungsten. The first shell contribution into the total EXAFS spectra was best-fitted using the regularization-like method [18]; the obtained RDFs $G(R)$ for W–O bonds at 10 and 300 K are shown in figure 3. RDF for α-$SnWO_4$ consists of two peaks centered at 1.82 and 2.15 Å: they correspond to the two groups of oxygen atoms (four and two) of the distorted WO_6 octahedron. The four nearest oxygen atoms are strongly bound, therefore the first peak in the RDF changes slightly upon increasing the temperature from 10 to 300 K. At the same time, the two distant oxygen atoms, contributing into the peak at 2.15 Å, are weakly bound, so that these two W–O bonds become longer at 300 K and the peak maximum shifts to 2.17 Å. In β-$SnWO_4$, RDF consists of only one narrow peak centered at 1.77 Å, being in agreement

Table 1. Comparison of the lattice parameters (a, b, c), the atomic fractional coordinates (x, y, z) and the unit cell volume (V_0), calculated using the LCAO method and determined from x-ray single-crystal diffraction [1, 2] for α-$SnWO_4$ ($Pnna$, no. 52, $Z = 4$) and β-$SnWO_4$ ($P2_13$, no. 198, $Z = 4$). E_g is the band gap.

	α-$SnWO_4$			β-$SnWO_4$	
	Experiment [1]	LCAO		Experiment [2]	LCAO
a (Å)	5.6270	5.5910		7.2989	7.3970
b (Å)	11.6486	11.6921			
c (Å)	4.9973	4.9934			
V_0 (Å^3)	327.56	326.42		388.84	404.74
Sn(z)	0.2196	0.2081	Sn(x, y, z)	0.8416	0.8316
W(x)	0.6677	0.6429	W(x, y, z)	0.1644	0.1645
O1(x)	0.3765	0.3547	O1(x, y, z)	0.3039	0.3022
O1(y)	0.2987	0.2976			
O1(z)	0.9988	0.9981			
O2(x)	0.1019	0.0846		0.8638	0.8614
O2(y)	0.3961	0.3969		0.7729	0.7736
O2(z)	0.6037	0.5975		0.5470	0.5504
E_g (eV)	1.64 [5]	1.45		2.68 [5], 2.7 [9], 2.6 [6]	4.36

with tetrahedral coordination of tungsten. Due to the rigidity of the WO_4 tetrahedra, the peak remains nearly unchanged upon heating to 300 K.

Next we will compare the results of our LCAO calculations, performed for a fully relaxed geometry, with the available experimental data. As one can see from table 1, the use of a hybrid functional allows one to obtain good agreement between experimental and theoretical values of the structural parameters and the indirect band gap for α-$SnWO_4$. However, the overestimated value of the lattice constant (by ~ 0.1 Å) and the larger value of the direct (at the X point of the Brillouin zone) band gap were found for β-$SnWO_4$. This disagreement can be related to the fact that the β-$SnWO_4$ phase is metastable at low temperatures. The larger band gap value in β-$SnWO_4$ is a consequence of the stronger crystal field splitting, caused by the shorter W–O bond length (figure 3).

The calculated partial density of electronic states (not shown) confirms a previous finding in [5, 6] on the origin of the valence and conduction bands. In both tungstates, the top of the valence band is mainly composed of the O 2p and Sn 5s states, whereas the conduction band originates mainly from the hybridized W 5d–O 2p states in α-$SnWO_4$, but Sn 5p states contribute additionally in β-$SnWO_4$.

To estimate the charge transfer effects, the atomic charges were obtained from Mulliken population analysis: $q(\mathrm{Sn}) = +1.52e$ ($+1.41e$), $q(\mathrm{W}) = +2.76e$ ($+2.62e$), $q(\mathrm{O1}) = -0.98e$ ($-0.96e$) and $q(\mathrm{O2}) = -1.16e$ ($-1.03e$) in α-$SnWO_4$ (β-$SnWO_4$). As one can see, all charges deviate from the formal (ionic) ones. The charge values suggest that the W–O bonds are largely covalent and the Sn–O bonds have some degree of covalency too. This fact explains the occurrence of the SOJT effects in WO_6 and SnO_6 octahedra [4, 6].

4. Conclusions

Low-temperature α-$SnWO_4$ and high-temperature metastable β-$SnWO_4$ tin tungstate phases were studied by the W L_3-edge x-ray absorption spectroscopy at 10 and 300 K. The EXAFS spectra were interpreted based on the results of the MS calculations. A detailed analysis of the EXAFS data from the first coordination shell of tungsten by the regularization-like method [18] allowed us to reconstruct the RDF within the first shell and to follow its temperature dependence. Strong distortion of the WO_6 octahedra was found in α-$SnWO_4$ and related to the SOJT effect. This conclusion was confirmed by the first-principles LCAO calculations, based on the hybrid exchange-correlation DFTl/HF scheme. Note that our total energy calculations provide a rather good agreement with the results of previous first-principles DFT calculations [5, 6] and known experimental data for both tungstate phases.

Acknowledgments

This work was supported by the Latvian Science Council grant no. 187/2012 and the European Social Fund within the project 2009/0138/1DP/1.1.2.1.2/09/IPIA/VIAA/004 ('Support for Doctoral Studies at the University of Latvia'). The experiments at DESY received funding from the European Community's Seventh Framework Programme (FP7/2007-2013) under grant agreement no. 226716.

References

[1] Jeitschko W and Sleight A W 1974 *Acta Crystallogr.* B **30** 2088
[2] Jeitschko W and Sleight A W 1972 *Acta Crystallogr.* B **28** 3174
[3] Solis J L, Frantti J, Lantto V, Häggström L and Wikner M 1998 *Phys. Rev.* B **57** 13491
[4] Kunz M and Brown I D 1995 *J. Solid State Chem.* **115** 395
[5] Cho I S, Kwak C H, Kim D W, Lee S and Hong K S 2009 *J. Phys. Chem.* C **113** 10647
[6] Stoltzfus M W, Woodward P M, Seshadri R, Klepeis J H and Bursten B 2007 *Inorg. Chem.* **46** 3839
[7] Zhu G, Que W, Zhang J and Zhong P 2011 *Mater. Sci. Eng.* B **176** 1448
[8] Huang R, Ge H, Lin X, Guo Y, Yuan R, Fua X and Li Z 2012 *RSC Adv.* **3** 1235
[9] Ungelenka J and Feldmann C 2012 *Chem. Commun.* **48** 7838
[10] Ungelenk J and Feldmann C 2012 *Appl. Catal.* B **127** 11
[11] Solis J L and Lantto V 1995 *Sensors Actuators* B **24–25** 591
[12] Solis J L and Lantto V 1997 *Phys. Scr.* **T69** 281

[13] Su Y, Hou L, Du C, Peng L, Guan K and Wang X 2012 *RSC Adv.* **2** 6266
[14] Rickers K, Drube W, Schulte-Schrepping H, Welter E, Brüggmann U, Herrmann M, Heuer J and Schulz-Ritter H 2007 *AIP Conf. Proc.* **882** 905
[15] Kuzmin A 1995 *Physica* B **208–209** 175
[16] Rehr J J and Albers R C 2000 *Rev. Mod. Phys.* **72** 621
[17] Aksenov V L, Kuzmin A Yu, Purans J and Tyutyunnikov S I 2001 *Phys. Part. Nuclei.* **32** 675
[18] Kuzmin A and Purans J 2000 *J. Phys.: Condens. Matter* **12** 1959
[19] Ankudinov A L, Ravel B, Rehr J J and Conradson S D 1998 *Phys. Rev.* B **58** 7565
[20] Hedin L and Lundqvist S 1971 *J. Phys.C: Solid State Phys.* **4** 2064
[21] Dovesi R *et al CRYSTAL09 User's Manual* (Turin: University of Turin)
[22] Kalinko A, Kuzmin A and Evarestov R A 2009 *Solid State Commun.* **149** 425
[23] Evarestov R A, Kalinko A, Kuzmin A, Losev M and Purans J 2009 *Integr. Ferroelectr.* **108** 1
[24] Kuzmin A, Kalinko A and Evarestov R A 2011 *Cent. Eur. J. Phys.* **9** 502
[25] Kuzmin A, Kalinko A and Evarestov R A 2013 *Acta Mater.* **61** 371
[26] Adamo C and Barone V 1999 *J. Chem. Phys.* **110** 6158
[27] Calatayud M, Andrés J and Beltrán A 1999 *Surf. Sci.* **430** 213
[28] Piskunov S, Heifets E, Eglitis R I and Borstel G 2004 *Comput. Mater. Sci.* **29** 165
[29] Monkhorst H J and Pack J D 1976 *Phys. Rev.* B **13** 5188
[30] Kuzmin A and Purans J 1993 *J. Phys.: Condens. Matter* **5** 9423
[31] Kuzmin A and Grisenti R 1994 *Phil. Mag.* B **70** 1161